Multiband envelope function model for quantum transport in a tunneling diode

Omar Morandi[1,*] and Michele Modugno[2]
[1]*Dipartimento di Elettronica e Telecomunicazioni, Università di Firenze, Via S. Marta 3, 50139 Firenze, Italy*
[2]*LENS—Dipartimento di Fisica and INFM, Università di Firenze, Via Nello Carrara 1, 50019 Sesto Fiorentino, Italy*
(Received 17 December 2004; revised manuscript received 16 March 2005; published 30 June 2005)

We present a simple model for electron transport in semiconductor devices that exhibit tunneling between the conduction and valence bands. The model is derived within the usual Bloch-Wannier formalism by a k expansion and is formulated in terms of a set of coupled equations for the electron envelope functions. Its connection with other models present in literature is discussed. As an application, we consider the case of a resonant interband tunneling diode, demonstrating the ability of the model to reproduce the expected behavior of the current as a function of the applied voltage.

DOI: 10.1103/PhysRevB.71.235331 PACS number(s): 73.40.−c, 85.30.Mn

I. INTRODUCTION

In recent years, there has been a growing interest for semiconductor devices characterized by tunneling effects between different bands, as the resonant interband tunneling diode (RITD).[1] This kind of diode belongs to the class of heterostructures that show a negative differential resistance in a certain range of the applied voltage, such as the widely employed RTD (resonant tunneling diode).[2,3] Unlike the latter where the electronic current flows within a single band, the remarkable feature of a RITD is the possibility to achieve a sharp coupling between "conduction" and "valence" states, allowing an interband current that becomes the main transport phenomena in the resonant region.

Hence, the description of electron transport in such quantum devices requires multiband models able to account for tunneling mechanisms between different bands induced by the heterostructure design and the applied external bias.

In the literature, different methods are currently employed for characterizing the band structures and the electronic or optical properties of these heterostructures, such as envelope functions, methods based on the effective mass theory,[4–6] tight-binding,[7,8] and pseudopotential[9] methods. In addition, various mathematical tools are employed to exploit the multiband quantum dynamics underlying the previous models: the Schrödinger-like models,[10] the nonequilibrium Green's function,[11,12] the Wigner function approach,[13–15] and recently the hydrodynamics multiband formalisms.[16,17]

All of these methods rely on some common approximations to account for the effects of a nonuniform band profile on the electron dynamics. In particular, in the usual $\mathbf{k}\cdot\mathbf{P}$ approach,[18] one starts by defining the Hamiltonian matrix of the bulk (in $\mathbf{k}$ space), and then allows the physical parameters (typically the band eigenvalues or the Luttinger-Kohn parameters)[19] to have some $\mathbf{x}$ dependence to describe the position-dependent properties of the heterostructure. In this approach, care must be taken to preserve the self-jointness of the Hamiltonian matrix, so appropriate quantization rules are needed.[20] In this way, the electrical fields arising from the band-edge offset among different layers are not included from the beginning in the derivation of the model, but appear only at the macroscopic level (i.e., at the level of envelope functions). Indeed, in the previous approximation technique, the $\mathbf{x}$ dependence of the unperturbed Hamiltonian matrix elements generates a mean effective electric field acting on the envelope functions, which is not present at the microscopic level.

A different approach has been proposed in Ref. 21 where a local modified Wannier basis is chosen to include the inhomogeneity directly into the basis elements. Unfortunately, in this case, the equations of motion of the envelope functions depend on the change of the Bloch functions across the interfaces (which are implicitly neglected in the previous procedure) and such an evaluation can result in a difficult task.

In this paper we discuss a different strategy, describing the band-edge offsets by means of external potentials applied to the bulk structure. This allows us to treat both the electrostatic potential generated by the charge distribution in the device and the heterostructure design of band edges on the same footing, which highlights the role played by the heterostructure potential in the interband tunneling process.

Within this framework we derive a hierarchy of multiband models obtained by means of a k expansion, where the momentum k plays the role of asymptotic parameter as in the usual $\mathbf{k}\cdot\mathbf{P}$ approach. The starting point is the single-electron Bloch representation, that here we consider for simplicity for the case of nondegenerate bands and constant band gaps. Then, after the k expansion, the electron wave function is projected on the Wannier basis, yielding a set of coupled Schrödinger equations for the electron envelope functions in definite energy bands.

These equations share some similarities with those of the well-known Kane[22] and Luttinger-Kohn (LK) (Ref. 19) models. However, a key difference is the choice of the basis elements. In a uniform crystal, the Wannier functions of a given energy band are related to the Bloch functions of the same band by a unitary transformation, which allows us to give a simple physical insight to the envelope functions. However, since the Kane model arises from a unitary transformation of only the periodic part of the Bloch functions, the generic element of the Kane basis is nondiagonal in the Bloch band index n, and envelope functions related to different band indices turn out to be coupled even in absence of any applied potential, therefore lacking of a direct physical interpretation.

The LK model instead is a multiband effective mass model obtained from the latter by an additional quasi-unitary transformation that removes the spurious interband coupling to first order in k. However, since the LK approach is devoted to describing intraband effects, the coupling due to the external field is generally neglected.

As an application of the present approach, we consider the case of a two-band RITD, showing that the model is able to reproduce the expected behavior of the current as a function of the applied voltage.

The paper is organized as follows. Section II discusses the derivation of the model and the approximations employed: Section III analyzes differences and analogies with the Kane[22] and Luttinger-Kohn[19] models. Finally, in Sec. IV, we work out explicitly the case of a RITD, investigating its current-voltage characteristic curve.

II. DERIVATION OF THE MODEL

Let us consider an electron of mass m immersed in a crystal lattice described by the periodic potential V_L, in the presence of an additional external potential U that will be treated as a perturbation. The evolution of the electron wave function $\Psi(\mathbf{x},t)$ is given by the solution of the Schrödinger equation

$$i\hbar\partial_t\Psi(\mathbf{x},t) = \left[-\frac{\hbar^2}{2m}\nabla^2 + V_L(\mathbf{x}) + U(\mathbf{x})\right]\Psi(\mathbf{x},t). \quad (1)$$

The eigenfunction of the unperturbed Hamiltonian $H_0 = -(\hbar^2/2m)\nabla^2 + V_L$ are Bloch functions $\psi_n(\mathbf{k},\mathbf{x})$ (e.g., see Ref. 18)

$$H_0\psi_n(\mathbf{k},\mathbf{x}) = E_n(\mathbf{k})\psi_n(\mathbf{k},\mathbf{x}) \quad (2)$$

and form a complete set with the orthonormality condition

$$\int_x \psi_n^*(\mathbf{k},\mathbf{x})\psi_{n'}(\mathbf{k}',\mathbf{x}) = \delta(\mathbf{k}-\mathbf{k}')\delta_{nn'}, \quad (3)$$

n being the band index and $\mathbf{k}$ the electron quasimomentum. Equation (1) can be transformed in momentum space by means of standard textbook methods[23,24] that we review below for completeness. According to the Bloch theorem, the Bloch functions $\psi_n(\mathbf{k},\mathbf{x})$ can be written as

$$\psi_n(\mathbf{k},\mathbf{x}) = e^{i\mathbf{k}\cdot\mathbf{x}}u_n(\mathbf{k},\mathbf{x}) \equiv \langle\mathbf{x}|n,\mathbf{k}\rangle, \quad (4)$$

where the functions $u_n(\mathbf{k},\mathbf{x})$ have the same periodicity of the lattice potential and are normalized according to

$$\frac{(2\pi)^3}{\Omega}\int_{\text{cell}} u_n^*(\mathbf{k},\mathbf{x})u_{n'}(\mathbf{k},\mathbf{x}) = \delta_{nn'}. \quad (5)$$

A generic solution of Eq. (1) can be expanded as

$$\Psi(\mathbf{x},t) = \sum_n \int_k \varphi_n(\mathbf{k},t)\psi_n(\mathbf{k},\mathbf{x}), \quad (6)$$

where $\mathbf{k}$ runs over the first Brillouin zone; then the expansion coefficients satisfy the following equation (hereinafter, we omit the time dependence to simplify the notation):

$$i\hbar\partial_t\varphi_n(\mathbf{k}) = E_n(\mathbf{k})\varphi_n(\mathbf{k}) + \sum_{n'}\int_{k'}\langle n,\mathbf{k}|U|n',\mathbf{k}'\rangle\varphi_{n'}(\mathbf{k}'). \quad (7)$$

By exploiting the periodicity of the $u_n(\mathbf{k},\mathbf{x})$ functions, the expectation value of the external potential U can be rewritten as[18]

$$\begin{aligned}\langle n,\mathbf{k}|U|n',\mathbf{k}'\rangle &= \int_x e^{i(\mathbf{k}'-\mathbf{k})\cdot\mathbf{x}}u_n^*(\mathbf{k},\mathbf{x})u_{n'}(\mathbf{k}',\mathbf{x})U(\mathbf{x}) \\ &= \sum_l B_l(n,n',\mathbf{k},\mathbf{k}')\int_x e^{i(\mathbf{k}'-\mathbf{k}-\mathbf{K}_l)\cdot\mathbf{x}}U(x) \\ &= (2\pi)^3\sum_l B_l\tilde{U}(\mathbf{k}'-\mathbf{k}-\mathbf{K}_l), \end{aligned} \quad (8)$$

$\mathbf{K}_l$ being a reciprocal lattice vector, and $\tilde{U}$ the Fourier transform of U.

At this point, following the discussion in Ref. 24, we assume the potential U to be nearly constant over a single lattice cell, so that only the zero momentum Fourier component gives a relevant contribution

$$\langle n,\mathbf{k}|U|n',\mathbf{k}'\rangle \simeq (2\pi)^3 B_0\tilde{U}(\mathbf{k}'-\mathbf{k}), \quad (9)$$

where B_0 can be expressed as

$$B_0 = \frac{1}{\Omega}\int_{\text{cell}} u_n^*(\mathbf{k},\mathbf{x})u_{n'}(\mathbf{k}',\mathbf{x}) \equiv \langle u_{n,\mathbf{k}}|u_{n',\mathbf{k}'}\rangle, \quad (10)$$

Ω being the volume of a single cell.

Let us now evaluate explicitly the coefficients B_0, by considering separately the case $n=n'$ and $n\neq n'$. In the former case it is easy to show from Eq. (3) that

$$B_0(n,n,\mathbf{k},\mathbf{k}') = 1/(2\pi)^3, \quad (11)$$

with the assumption that both $\mathbf{k}$ and $\mathbf{k}'$ lie within the first Brillouin zone so that their difference is not a reciprocal lattice vector.[18]

The case $n\neq n'$ can be carried out by considering the eigenvalue equation for the $u_n(\mathbf{k},\mathbf{x})$ functions

$$\bar{H}_0(\mathbf{k})|u_{n,\mathbf{k}}\rangle = E_n(\mathbf{k})|u_{n,\mathbf{k}}\rangle, \quad (12)$$

where we have defined $\bar{H}_0(\mathbf{k})$ as ($\hat{\mathbf{p}} \equiv -i\hbar\boldsymbol{\nabla}$)

$$\bar{H}_0(\mathbf{k}) \equiv \frac{1}{2m}(\hat{\mathbf{p}} + \hbar\mathbf{k})^2 + V_L(\mathbf{x}). \quad (13)$$

Then, by left multiplying Eq. (12) by $\langle u_{n',\mathbf{k}'}|$ and using the equivalence

$$\bar{H}_0(\mathbf{k}) = \bar{H}_0(\mathbf{k}') + \frac{\hbar^2}{2m}(k^2-k'^2) + \frac{\hbar}{m}\hat{\mathbf{p}}\cdot(\mathbf{k}-\mathbf{k}'), \quad (14)$$

we get

$$B_0(n,n'\neq n,\mathbf{k},\mathbf{k}') = \frac{\hbar}{m}(\mathbf{k}-\mathbf{k}')\frac{\mathbf{P}_{nn'}(\mathbf{k},\mathbf{k}')/(2\pi)^3}{\Delta E_{nn'}(\mathbf{k},\mathbf{k}')}, \quad (15)$$

with the momentum matrix elements $P_{nn'}(\mathbf{k},\mathbf{k}')$ defined by

$$\mathbf{P}_{nn'}(\mathbf{k},\mathbf{k}') \equiv \frac{(2\pi)^3}{\Omega}\int_{\text{cell}} u_n^*(\mathbf{k},\mathbf{x})(-i\hbar\,\boldsymbol{\nabla})u_{n'}(\mathbf{k}',\mathbf{x}) \quad (16)$$

and

$$\Delta E_{nn'}(\mathbf{k},\mathbf{k}') \equiv E_n(\mathbf{k}) - E_{n'}(\mathbf{k}') - \frac{\hbar^2}{2m}(k^2 - k'^2). \quad (17)$$

Finally, Eq. (7) for the expansion coefficients can be rewritten as

$$i\hbar\partial_t\varphi_n(\mathbf{k}) = E_n(\mathbf{k})\varphi_n(\mathbf{k}) + \int_{k'}\widetilde{U}(\mathbf{k}-\mathbf{k}')\varphi_n(\mathbf{k}') + \frac{\hbar}{m}\sum_{n'\neq n}\int_{k'}\frac{\mathbf{P}_{nn'}(\mathbf{k},\mathbf{k}')}{\Delta E_{nn'}(\mathbf{k},\mathbf{k}')}(\mathbf{k}-\mathbf{k}') \times\widetilde{U}(\mathbf{k}-\mathbf{k}')\varphi_{n'}(\mathbf{k}'), \quad (18)$$

where it is easy to identify the single-band dynamics (first line) and the interband coupling (second line). This equation is general and relies on the assumption that the external potential U has no appreciable variation on the scale of a single lattice cell [see Eq. (9)].

Let us now transform back the above equation in coordinate space; this can be achieved by projection on the Wannier basis

$$\Psi(\mathbf{x}) = \sum_n\sum_{\mathbf{R}_i}\chi_n(\mathbf{R}_i)\phi_n^W(\mathbf{x}-\mathbf{R}_i), \quad (19)$$

where the Wannier basis functions satisfy the orthogonality relation

$$\int_x \phi_n^{W*}(\mathbf{x}-\mathbf{R}_i)\phi_{n'}^W(\mathbf{x}-\mathbf{R}_j) = \delta_{nn'}\delta_{ij} \quad (20)$$

and can be expressed in terms of Bloch functions as

$$\phi_n^W(\mathbf{x}-\mathbf{R}_i) = \sqrt{\frac{\Omega}{(2\pi)^3}}\int_k \psi_n(\mathbf{k},\mathbf{x}-\mathbf{R}_i). \quad (21)$$

The use of the Wannier basis has two advantages. (i) The amplitudes $\chi_n(\mathbf{R}_i)$, that play the role of envelope functions on the new basis [see Eq. (19)] can be obtained from the Bloch coefficients in Eq. (18) by a simple Fourier transform

$$\chi_n(\mathbf{R}_i) = \sqrt{\frac{\Omega}{(2\pi)^3}}\int_k \varphi_n(\mathbf{k})e^{i\mathbf{k}\cdot\mathbf{R}_i}. \quad (22)$$

(ii) They can be interpreted as the actual wave function of an electron in the nth band if one is interested in macroscopic properties of the system on a scale much larger than the lattice spacing (that is equivalent to average on a scale of the order of the lattice cell). For example, by using the completeness of the Wannier basis in Eq. (20), the density and current distributions can be expressed as

$$\bar{\rho}_i \equiv \langle\rho(\mathbf{x})\rangle_{\text{cell}-i} \simeq \sum_n |\chi_n(\mathbf{R}_i)|^2, \quad (23)$$

$$\bar{\mathbf{J}}_i \equiv \langle\mathbf{J}(\mathbf{x})\rangle_{\text{cell}-i} \simeq \frac{\hbar}{im}\text{Im}\sum_n[\chi_n^*(\mathbf{R}_i)\,\boldsymbol{\nabla}\,\chi_n(\mathbf{R}_i)]. \quad (24)$$

Since the functions $\chi_n(\mathbf{R}_i)$, in principle, are defined only at the lattice sites, it is convenient to follow the approach of Ref. 25 and perform the limit to the continuum by extending the dependence of the $\chi_n(\mathbf{R}_i)$ to the whole space ($\mathbf{R}_i\to\mathbf{x}$). This yields the following expressions for the cell-averaged charge and current densities

$$\bar{\rho}(\mathbf{x}) \simeq \sum_n |\chi_n(\mathbf{x})|^2, \quad (25)$$

$$\bar{\mathbf{J}}(\mathbf{x}) \simeq \frac{\hbar}{im}\text{Im}\sum_n[\chi_n^*(\mathbf{x})\,\boldsymbol{\nabla}\,\chi_n(\mathbf{x})]. \quad (26)$$

Then, by using standard properties of the Fourier transform, Eq. (18) can be formally written in coordinate space as

$$i\hbar\partial_t\chi_n(\mathbf{x}) = E_n(-i\hbar\,\boldsymbol{\nabla})\chi_n(\mathbf{x}) + U(\mathbf{x})\chi_n(\mathbf{x}) + \frac{\hbar}{m}\sum_{n'\neq n}\sqrt{\frac{\Omega}{(2\pi)^3}}\int_k e^{i\mathbf{k}\cdot\mathbf{x}}\int_{k'}\frac{\mathbf{P}_{nn'}(\mathbf{k},\mathbf{k}')}{\Delta E_{nn'}(\mathbf{k},\mathbf{k}')} \times(\mathbf{k}-\mathbf{k}')\widetilde{U}(\mathbf{k}-\mathbf{k}')\varphi_{n'}(\mathbf{k}'). \quad (27)$$

This equation is equivalent to the generalized form of the Wannier equations of Ref. 25, with the advantage of having the interband term written in a more transparent form in terms of its Fourier components. This expression allows for a simple manipulation of the above equation, which for practical use has to be further simplified. The simplest approach is to adopt the following standard approximations,[26] assuming that (i) the energy spectrum is of simple form with minima (maxima) of each band at some point $\boldsymbol{k}=\boldsymbol{k}_0$ in the first Brillouin zone; (ii) the $\varphi_n(\mathbf{k})$ functions are localized on a small region of $\boldsymbol{k}$ space around $\boldsymbol{k}=\boldsymbol{k}_0$ during the whole evolution of the system. For convenience in the notations, and without loss of generality, in the rest of the paper we will set $\boldsymbol{k}_0=0$. Then let us consider the term $\mathbf{P}_{nn'}(\mathbf{k},\mathbf{k}')/\Delta E_{nn'}(\mathbf{k},\mathbf{k}')$ that characterizes the interband coupling; to first order in k, k' we can write

$$\frac{\mathbf{P}_{nn'}(\mathbf{k},\mathbf{k}')}{\Delta E_{nn'}(\mathbf{k},\mathbf{k}')} = \frac{\mathbf{P}_{nn'}}{\Delta E_{nn'}} + \frac{1}{\Delta E_{nn'}}\left(\mathbf{k}\cdot\boldsymbol{\nabla}_k\mathbf{P}_{nn'} + \mathbf{k}'\cdot\boldsymbol{\nabla}_{k'}\mathbf{P}_{nn'}\right) + O(k^2), \quad (28)$$

where to simplify the notation we have defined $\Delta E_{nn'} = \Delta E_{nn'}(\mathbf{0},\mathbf{0}) = E_n(\mathbf{0}) - E_{n'}(\mathbf{0}) \equiv E_n - E_{n'}$, $\mathbf{P}_{nn'} = \mathbf{P}_{nn'}(\mathbf{0},\mathbf{0})$, and we have used the fact that the energies do not contain first-order terms in $\mathbf{k}$ [see (ii)].

The first derivatives in Eq. (28) can be evaluated by using the relation

$$\boldsymbol{\nabla}_k u_n(\mathbf{k},\mathbf{x}) = \frac{\hbar}{m}\sum_{n'\neq n} u_{n'}(\mathbf{k},\mathbf{x})\frac{\mathbf{P}_{n'n}(\mathbf{k},\mathbf{k})}{E_n(\mathbf{k}) - E_{n'}(\mathbf{k})} \quad (29)$$

that can be obtained by differentiation of Eq. (12) with respect to $\mathbf{k}$, and projecting the term $\boldsymbol{\nabla}_k u_n(\mathbf{k},\mathbf{x})$ on the $u_n(\mathbf{k},\mathbf{x})$ basis.[25] Then a straightforward calculation yields

$$\nabla_k \mathbf{P}_{nn'} = \frac{\hbar}{m} \sum_{n'' \neq n} \frac{\mathbf{P}_{nn''}\mathbf{P}_{n''n'}}{E_n - E_{n''}} \equiv M_{nn'}, \tag{30}$$

$$\nabla_{k'} \mathbf{P}_{nn'} = \frac{\hbar}{m} \sum_{n'' \neq n'} \frac{\mathbf{P}_{nn''}\mathbf{P}_{n''n'}}{E_{n'} - E_{n''}} = M^*_{n'n}, \tag{31}$$

where $\mathbf{P}^*_{n'n}(\mathbf{k},\mathbf{k}') = \mathbf{P}_{nn'}(\mathbf{k},\mathbf{k}')$. The last term of Eq. (27) then becomes

$$\begin{aligned}
&\int_{k'} \frac{\mathbf{P}_{nn'}(\mathbf{k},\mathbf{k}')}{\Delta E_{nn'}(\mathbf{k},\mathbf{k}')} \times (\mathbf{k}-\mathbf{k}')\tilde{U}(\mathbf{k}-\mathbf{k}')\varphi_{n'}(\mathbf{k}') \\
&= \frac{\hbar}{m} \sum_{n' \neq n} \frac{\mathbf{P}_{nn'}}{\Delta E_{nn'}} \int_{k'} (\mathbf{k}-\mathbf{k}')\tilde{U}(\mathbf{k}-\mathbf{k}')\varphi_{n'}(\mathbf{k}') \\
&+ \frac{\hbar}{m} \sum_{n' \neq n} \frac{M^*_{n'n}}{\Delta E_{nn'}} \int_{k'} (\mathbf{k}-\mathbf{k}')\tilde{U}(\mathbf{k}-\mathbf{k}')\mathbf{k}'\varphi_{n'}(\mathbf{k}') \\
&+ \mathbf{k}\frac{\hbar}{m} \sum_{n' \neq n} \frac{M_{nn'}}{\Delta E_{nn'}} \int_{k'} (\mathbf{k}-\mathbf{k}')\tilde{U}(\mathbf{k}-\mathbf{k}')\varphi_{n'}(\mathbf{k}') + o(\mathbf{k}^2).
\end{aligned} \tag{32}$$

This expression allows us to write Eq. (27) as

$$\begin{aligned}
i\hbar\partial_t \chi_n(\mathbf{x}) &= E_n(-i\hbar\nabla)\chi_n(\mathbf{x}) + U(\mathbf{x})\chi_n(\mathbf{x}) \\
&- i\nabla U(\mathbf{x}) \frac{\hbar}{m} \sum_{n' \neq n} \frac{\mathbf{P}_{nn'}}{\Delta E_{nn'}} \chi_{n'}(\mathbf{x}) \\
&- \nabla U(\mathbf{x}) \frac{\hbar}{m} \sum_{n' \neq n} \frac{M^*_{n'n}}{\Delta E_{nn'}} \nabla \chi_{n'}(\mathbf{x}) \\
&- \frac{\hbar}{m} \sum_{n' \neq n} \frac{M_{nn'}}{\Delta E_{nn'}} [\nabla^2 U(\mathbf{x})\chi_{n'}(\mathbf{x}) \\
&+ \nabla U(\mathbf{x}) \nabla \chi_{n'}(\mathbf{x})].
\end{aligned} \tag{33}$$

Equation (33) represents the main result of this paper. It describes the evolution of the Wannier envelope functions by fully including the effects of the periodic potential and accounting for the interband coupling due to the perturbation potential U up to second order in k. Equation (33) can be further simplified by means of the usual effective mass approximation that amounts to retaining only up to quadratic terms in k in the kinetic operator. In general, this corresponds to replacing the bare mass with a 3×3 mass tensor m^*_{ij}[23]; in the special case of an isotropic periodic potential or for a one-dimensional system as we will consider later, one simply gets

$$E_n(\mathbf{k}) = E_n + \frac{\hbar^2 k^2}{2m^*_n} + O(k^3). \tag{34}$$

III. COMPARISON WITH OTHER k·P MODELS

Let us now discuss the connection of the model in Eq. (33) with other two $\mathbf{k}\cdot\mathbf{P}$ models, namely the Kane and LK models,[19,22] which are widely used both to estimate the band diagram in semiconductor and the transmission coefficients of interband devices.[27–29]

The Kane model is based on the following choice of the basis elements

$$\langle \mathbf{x}|n,\mathbf{k}\rangle_{\mathrm{Ka}} \equiv e^{i\mathbf{k}\cdot\mathbf{x}} u_n(\mathbf{0},\mathbf{x}), \tag{35}$$

which form a complete orthonormal set, and can be used to expand the electron wave function Ψ in a way similar to that shown in Sec. II. On this basis, the Schrödinger equation takes the form

$$i\hbar\partial_t \varphi_n(\mathbf{k}) = \sum_{n'} \int_{k'} \mathcal{H}^{\mathrm{Ka}}_{nn'}(\mathbf{k},\mathbf{k}')\varphi_{n'}(\mathbf{k}'), \tag{36}$$

where the Hamiltonian matrix elements are

$$\begin{aligned}
\mathcal{H}^{\mathrm{Ka}}_{nn'}(\mathbf{k},\mathbf{k}') &\equiv \langle n,\mathbf{k}|H_0 + U|n',\mathbf{k}'\rangle_{\mathrm{Ka}} \\
&= \left[\left(E_n + \frac{\hbar^2 k^2}{2m_0}\right)\delta_{nn'} + \frac{\hbar}{m_0}\mathbf{k}\cdot\mathbf{P}_{nn'}\right]\delta(\mathbf{k}-\mathbf{k}') \\
&+ \tilde{U}(\mathbf{k}-\mathbf{k}')\delta_{nn'}.
\end{aligned} \tag{37}$$

By means of an inverse Fourier transform [see Eq. (22)] it is straightforward to recover the equation for Kane envelope functions $\chi^{\mathrm{Ka}}_n(\mathbf{x})$

$$\begin{aligned}
i\hbar\partial_t \chi^{\mathrm{Ka}}_n(\mathbf{x}) &= \left(-\frac{\hbar^2}{2m}\nabla^2 + E_n + U(\mathbf{x})\right)\chi^{\mathrm{Ka}}_n(\mathbf{x}) \\
&- i\frac{\hbar}{m} \sum_{n' \neq n} \mathbf{P}_{nn'} \cdot \nabla \chi^{\mathrm{Ka}}_{n'}(\mathbf{x}).
\end{aligned} \tag{38}$$

This equation shows that in the Kane representation, envelope functions related to different band indices are coupled even if the external field is vanishing. This is due to the fact that the unperturbed Hamiltonian H_0 is not diagonal on the Kane basis [see Eq. (37)]; therefore, the n here does not correspond to the usual band index of the Bloch picture. In other words, this means that the envelope functions $\chi^{\mathrm{Ka}}_n(\mathbf{x})$ do not have the direct physical meaning of wave functions of an electron in a definite energy band. As a consequence, one should be careful in estimating truncation errors when the full problem is reduced to a finite set of envelope functions.

To overcome the previous difficulty, Luttinger and Kohn proposed a different choice of the basis functions.[19] The idea is to use a quasi-unitary transformation Θ to diagonalize the Kane Hamiltonian in the momentum space up to first order in k. In this way, it is possible to get a natural extension of the effective mass single-band model in the multiband framework. The new Hamiltonian reads

$$\mathcal{H}^{\mathrm{LK}} = \Theta^{-1}\mathcal{H}^{\mathrm{Ka}}\Theta, \tag{39}$$

where Θ is defined as follows

$$\langle n,\mathbf{k}|\Theta|n',\mathbf{k}'\rangle_{\mathrm{Ka}} = \left(\delta_{nn'} - \frac{\hbar}{m_0}\frac{\mathbf{P}_{nn'}\cdot\mathbf{k}}{\Delta E_{nn'}}\right)\delta(\mathbf{k}-\mathbf{k}'), \tag{40}$$

providing a unitary transformation to first order in k. Accordingly, the elements of the LK basis are defined by $|n,\mathbf{k}\rangle_{\mathrm{LK}}$

$=\Theta|n,\mathbf{k}\rangle_{\mathrm{Ka}}$, and correspond to an expansion of the $u_n(\mathbf{k},\mathbf{x})$ functions to first order in k

$$\langle \mathbf{x}|n,\mathbf{k}\rangle_{\mathrm{LK}} = e^{i\mathbf{k}\cdot\mathbf{x}}\left[u_n(\mathbf{0},\mathbf{x}) + \mathbf{k}\frac{\partial u_n(\mathbf{0},\mathbf{x})}{\partial \mathbf{k}}\bigg|_{\mathbf{0}}\right]. \quad (41)$$

In the coordinate space, the LK model reads

$$\begin{aligned} i\hbar\partial_t \chi_n^{\mathrm{LK}}(\mathbf{x}) &= \left[E_n - \frac{\hbar^2}{2m_n^*}\nabla^2 + U(\mathbf{x})\right]\chi_n^{\mathrm{LK}}(\mathbf{x}) \\ &\quad - i\,\boldsymbol{\nabla}\, U(\mathbf{x})\frac{\hbar}{m}\sum_{n'\neq n}\frac{\mathbf{P}_{nn'}}{\Delta E_{nn'}}\chi_{n'}^{\mathrm{LK}}(\mathbf{x}) \\ &\quad + \frac{\hbar}{m_0}\sum_{n''n'\neq n}\left(\mathbf{P}_{nn''}\boldsymbol{\nabla}\right)\left(\mathbf{P}_{n''n'}\boldsymbol{\nabla}\right) \\ &\quad \times\left(\frac{1}{\Delta E_{nn''}} - \frac{1}{\Delta E_{n''n'}}\right)\chi_{n'}^{\mathrm{LK}}(\mathbf{x}). \end{aligned} \quad (42)$$

The first line here corresponds to the first line of Eq. (33) with the effective mass approximation [see Eq. (34)]; the second line instead represents a spurious coupling between different bands that corresponds to the choice of the truncated basis in Eq. (41) and is usually neglected.[18] In our approach, this term would come from the expansion of the off-diagonal kernel

$$\langle n,\mathbf{k}|H_0|n',\mathbf{k}'\rangle = \int_x e^{-i\mathbf{k}\cdot\mathbf{x}}u_n^*(\mathbf{k},\mathbf{x})H_0 e^{i\mathbf{k}\cdot\mathbf{x}}u_{n'}(\mathbf{k}',\mathbf{x}), \quad (43)$$

but is canceled exactly by a term coming from the expansion of the $u_n(\mathbf{k},\mathbf{x})$ functions to second order in k. As a matter of fact, this contribution is absent in our approach since only the off-diagonal terms that depend on the external potential U have been approximated [up to $O(k^2)$ in Eq. (33)].

We also remark that in the LK approach, one usually neglects the interband coupling proportional to the applied field ∇U, and this prevents any description of interband tunneling effects.

IV. AN EXAMPLE

As an application of the model discussed in Sec. II, we consider a one-dimensional semiconductor device consisting of a multilayer heterostructure where only two bands play a relevant role, namely the conduction and valence bands. As a further approximation, we keep the interband terms only to first order in k, neglecting the terms proportional to the matrix $M_{nn'}$, and adopt the effective mass approximation of Eq. (34). Thus the system in Eq. (33) can be reduced to the following set of coupled equations:

$$\begin{aligned} i\hbar\partial_t\chi_c(x) &= E_c\chi_c(x) - \frac{\hbar^2}{2m_c^*}\nabla^2\chi_c(x) + U(x)\chi_c(x) \\ &\quad - i\,\nabla\, U(x)\frac{\hbar P}{mE_g}\chi_v(x), \end{aligned}$$

$$\begin{aligned} i\hbar\partial_t\chi_v(x) &= E_v\chi_v(x) + \frac{\hbar^2}{2|m_v^*|}\nabla^2\chi_v(x) + U(x)\chi_v(x) \\ &\quad - i\,\nabla\, U(x)\frac{\hbar P}{mE_g}\chi_c(x), \end{aligned} \quad (44)$$

that depend on four phenomenological parameters: the interband momentum matrix $P\equiv P_{c,v}=P_{v,c}^*$ (see Refs. 10 and 24 for a numerical estimate), the energy gap $E_g\equiv E_c-E_v$, and the effective masses $m_{c,v}^*$ for the conduction and valence bands, respectively ($m_v^*=-|m_v^*|$).

The total potential can be written as $U(x)=U_h(x)+U_e(x)$, where $U_e(x)$ is the electrostatic potential generated by the charge distribution in the device, and $U_h(x)$ accounts for the spatial dependence of the band edges in the heterostructure. Indeed, in real heterostructures, the conduction and valence band edges depend on x. To account for this, we consider the Bloch spectrum as constant among the layers, treating the actual spatial dependence as an external potential applied to the heterostructure bulk. We also remark here that we are considering only coherent transport, neglecting any dissipative phenomena like electron-phonon scattering that are not expected to affect significantly the tunneling process.

The electrostatic potential can be calculated self-consistently by using the Poisson equation

$$\epsilon\nabla^2 U_e(x) = q\rho(x) = q^2[C(x)-n(x)], \quad (45)$$

where the total charge distribution $\rho(x)$ is the sum of the charge concentration $qC(x)$ of the doping ions plus the charge distribution $-qn(x)$ of free electrons.

Let us now consider a heterostructure device in contact with a source and a drain reservoir at temperature T. In the presence of an incident electron beam with momentum q and energy $E(q)$ injected from the reservoirs into the device, the steady state of the system is obtained from the solution of the stationary equations

$$\begin{aligned} E(q)\chi_c^q(x) &= E_c\chi_c^q(x) - \frac{\hbar^2}{2m_c^*}\nabla^2\chi_c^q(x) + U(x)\chi_c^q(x) \\ &\quad - i\,\nabla\, U(x)\frac{\hbar P}{mE_g}\chi_v^q(x), \end{aligned}$$

$$\begin{aligned} E(q)\chi_v^q(x) &= E_v\chi_v^q(x) + \frac{\hbar^2}{2|m_v^*|}\nabla^2\chi_v^q(x) + U(x)\chi_v^q(x) \\ &\quad - i\,\nabla\, U(x)\frac{\hbar P}{mE_g}\chi_c^q(x) \end{aligned} \quad (46)$$

combined with the Poisson equation [Eq. (45)]. The equations are solved by approximating the spatial derivative by a Runge-Kutta method and using a Gummel predictor scheme to reach convergence.[30]

The electronic density $n=n_c+n_v$ is constructed in terms of the pure state solutions χ_c^q and χ_v^q of the above equations, weighted by the momentum distribution of the incident beams

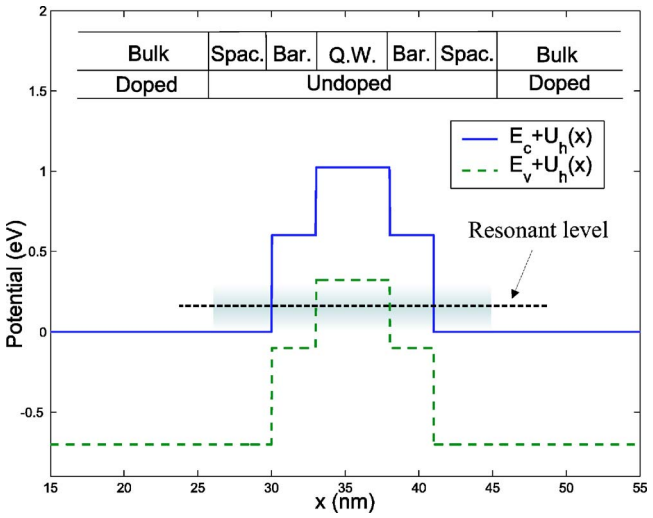

FIG. 1. (Color online) Simulated heterostructure profile and doped regions of the RITD. The widths of the layers are chosen: 5.00 nm for the quantum well (Q.W.), 3.00 nm for the barriers (Bar.), and 4.50 nm for the spacer layers (Spac.). Resonant tunneling takes place when the energy of electrons in the conduction band is resonant with that of the bounded hole state in the central quantum well (shaded area).

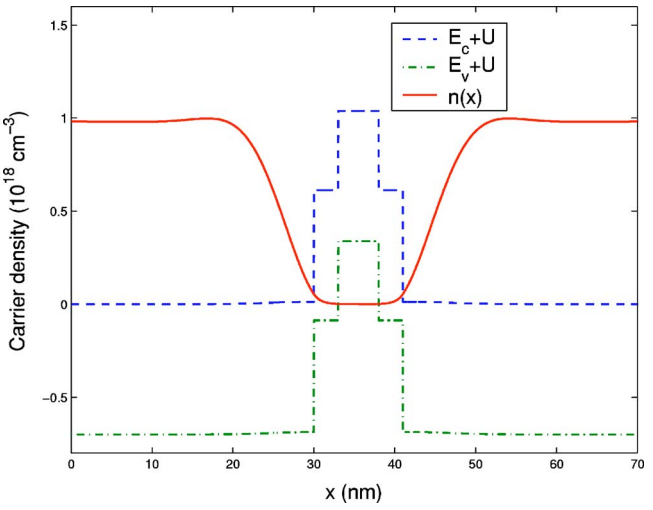

FIG. 2. (Color online) Self-consistent potential profile and density of electrons corresponding to unbiased case.

$$n(x) = \int_0^\infty dq\, f_0(q)[|\chi_c^q(x)|^2 + |\chi_v^q(x)|^2], \tag{47}$$

where $f_0(q)$ is the Fermi-Dirac distribution integrated on the transverse coordinates.[31]

Similarly, the electronic current $J=J_c+J_v$ is calculated as

$$J(x) = \sum_{i=c,v} \frac{\hbar}{2m_i} \int_0^\infty dq\, f_0(q) \mathrm{Im}[\chi_i^q(x) \nabla \chi_i^q(x)]. \tag{48}$$

To model the charge injected in the device from the source and drain reservoirs, we use transparent boundary conditions. For example, at $x=0$, in the case of an electron beam incident in the conduction band with positive momentum q, we have

$$\frac{d}{dx} \begin{pmatrix} \chi_c^q \\ \chi_v^q \end{pmatrix} \Bigg|_{x=0} = \begin{pmatrix} -ik_i & 0 \\ 0 & -ik_r \end{pmatrix} \begin{pmatrix} \chi_c^q \\ \chi_v^q \end{pmatrix} + \begin{pmatrix} 2ik_i \\ 0 \end{pmatrix}, \tag{49}$$

where

$$k_i = \sqrt{\frac{2m_c^*}{\hbar^2}[E(q) - E_c]}, \tag{50}$$

$$k_r = -i\sqrt{\frac{2|m_v^*|}{\hbar^2}[E(q) - E_v]}; \tag{51}$$

the other cases are treated in similar way.

Let us now discuss what happens in the case of a one-dimensional RITD, where charge transport across the device takes place thanks to resonant tunneling between electron states in the conduction band and hole states in the valence band. As a specific case, here we consider the simple test device depicted in Fig. 1, consisting of a 5.00-nm-wide quantum well (for hole states), bounded by two identical 3.00-nm-wide barriers that are interfaced to the bulk by two 4.50-nm-wide spacer layers. In Fig. 1 we also show the resulting heterostructure potential in the case of a GaSb lattice bulk with a doping concentration of 10^{18} cm^{-3} (Ref. 32). For consistency with the formalism presented in the previous sections, we are considering a constant band gap heterostructure (note that, in our model, all the interband effects are taken in account by an external potential added to the bulk Hamiltonian). We note that, as far as resonant tunneling is concerned, the actual shape of the conduction band far above the resonance level cannot produce strong effects on the tunneling process. Therefore, we expect that the *I-V* behavior will not change qualitatively in cases of more complex conduction bands profiles.

In Fig. 2 we show the calculated equilibrium self-consistent potential U and the density of electrons corresponding to the unbiased case: note that, in this case, the profile of the heterostructure potential U_h of Fig. 1 is practically unchanged by the addition of the electrostatic potential U_e.

The steady *I-V* characteristic of the device at a temperature of 300 K is shown in Fig. 3, where the current I flowing through the device is plotted as a function of the bias voltage V_b applied to the drain contact. This picture shows that the model is able to reproduce the expected negative differential resistance (NDR) in a certain range of values of the applied potential (here for $V_b > V_0 = 0.225$ V).

In Fig. 4 we show the calculated self-consistent potential profile U and the density of electrons corresponding to peak and valley currents, for $V_b = 0.225$ V and $V_b = 0.27$ V, respectively. We note that as expected, the density of electrons in the central region of the potential profile (see Fig. 4) is an increasing function of the applied bias below resonance ($V_b < V_0$), which then sharply decreases in the NDR region.

These results demonstrate that the present model is as promising for reproducing the *I-V* curves of physical devices as that considered, for example, in Refs. 33 and 34, although a precise comparison requires the extension of the model to

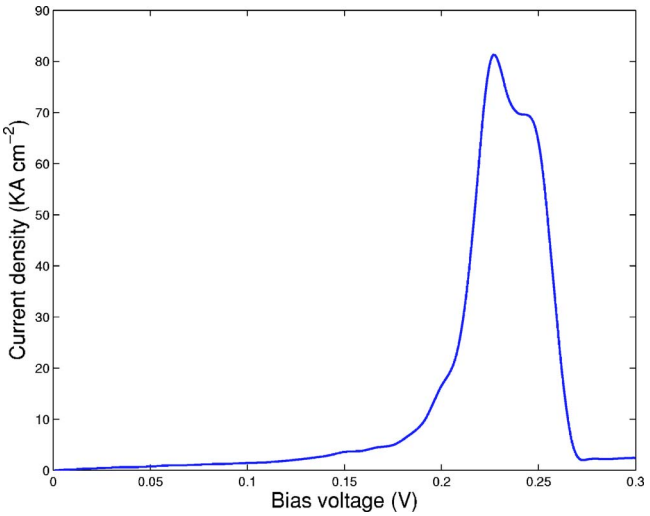

FIG. 3. (Color online) I-V characteristic of the simulated diode. Notice the negative differential resistance for $V_b > V_0 = 0.05$ V.

structures with varying band gap profiles (or, more generally, with x-dependent Luttinger-Kohn parameters[20]) and will be considered in a future publication.

V. CONCLUSIONS

We have presented a multiband model for electron transport in a crystal lattice. The model is derived within the usual Bloch theory by means of a k expansion and is formulated in terms of cell-averaged envelope functions obtained by projection in the Wannier representation. The model is suited to describe, in a clear fashion, tunneling effects between different bands in the presence of an applied potential. Its advantages with respect to other widely used approaches have been discussed.

As an application, we have considered the case of a RITD, a heterostructure device where the electronic current flows between a conduction and a valence band, interfaced by potential barriers. In this case the model is reduced to a system of two Schrödinger equations for the electron envelope function coupled with the Poisson equation for the field generated by the electronic distribution itself. It nicely reproduces the expected behavior of the current as a function of the applied voltage, exhibiting a negative differential resistance in a certain range of values of the applied bias.

The present approach is, therefore, particularly promising for reproducing the behavior of physical devices characterized by resonant tunneling, and we are currently working at extending the model in order to take into account the specific symmetry properties of the crystal lattice and to treat degenerate and varying band gap profiles. Moreover, with the inclusion of spin-orbit coupling, our model may also be relevant for the field of spintronics, where $\mathbf{k}\cdot\mathbf{P}$ methods are becoming increasingly important.[35,36]

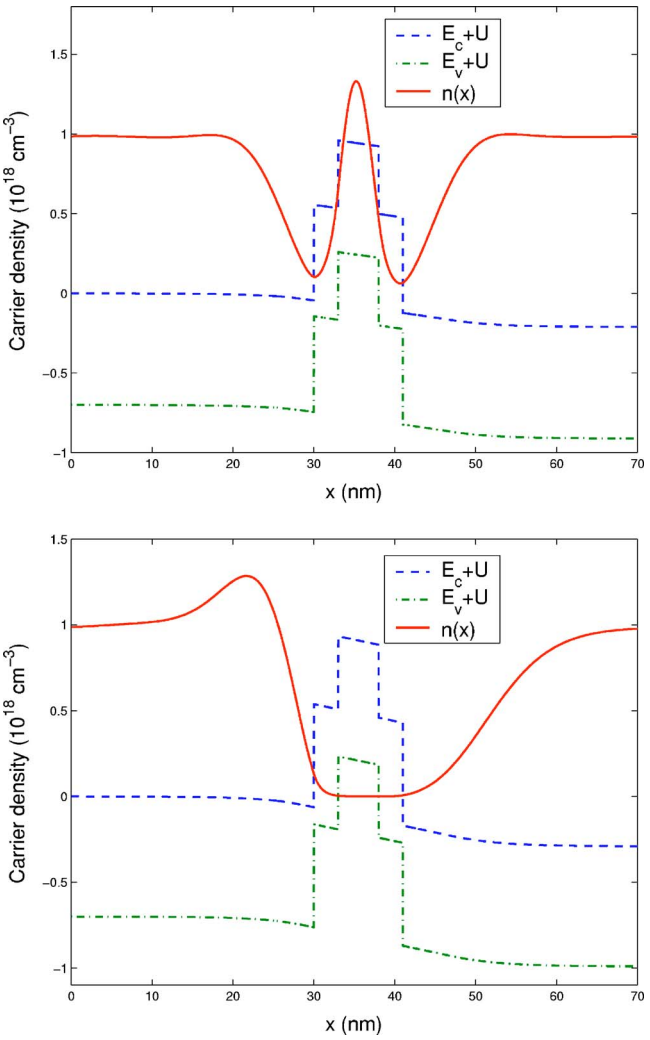

FIG. 4. (Color online) Self-consistent potential profile and density of electrons corresponding to the peak (top) and to the valley (bottom) currents.

ACKNOWLEDGMENTS

We thank G. Frosali, G. Borgioli, J. Kefi, and N. Ben Abdallah for many stimulating discussions. O. M. acknowledges hospitality from the MIP laboratory of the P. Sabatier University of Toulouse.

*Corresponding author. Electronic address: omar.morandi@unifi.it

[1] J. Genoe, K. Fobelets, C. Van Hoof, and G. Borghs, Phys. Rev. B **52**, 14025 (1995); R. Q. Yang and J. M. Xu, J. Appl. Phys. **15**, 4714 (1992).

[2] N. C. Kluksdahl, A. M. Kriman, D. K. Ferry, and C. Ringhofer, Phys. Rev. B **39**, 7720 (1989).

[3] F. A. Buot and K. L. Jensen, Phys. Rev. B **42**, 9429 (1990).

[4] Y. X. Liu, D. Z. Y. Ting, and T. C. McGill, Phys. Rev. B **54**, 5675

(1996).
[5] C. Y. P. Chao and S. L. Chuang, Phys. Rev. B **43**, 7027 (1991).
[6] D. Z. Y. Ting, E. T. Yu, and T. C. McGill, Phys. Rev. B **45**, 3583 (1992).
[7] T. B. Boykin, J. P. A. van der Wagt, and J. S. Harris, Jr., Phys. Rev. B **43**, 4777 (1991).
[8] R. C. Bowen, W. R. Frensley, G. Klimeck, and R. K. Lake, Phys. Rev. B **52**, 2754 (1995).
[9] G. B. Bachelet, D. R. Hamann, and M. Schlüter, Phys. Rev. B **26**, 4199 (1982).
[10] M. Sweeney and J. M. Xu, Appl. Phys. Lett. **54**, 546 (1989).
[11] R. Lake, G. Klimeck, R. C. Bowen, and D. Jovanovic, J. Appl. Phys. **81**, 7845 (1997).
[12] R. Lake and S. Datta, Phys. Rev. B **45**, 6670 (1992).
[13] G. Borgioli, G. Frosali, and P. F. Zweifel, Transp. Theory Stat. Phys. **32**, 347 (2003).
[14] L. Demeio, L. Barletti, A. Bertoni, P. Bordone, and C. Jacoboni, Physica B **314**, 104 (2002).
[15] L. Demeio, P. Bordone, and C. Jacoboni, Semicond. Sci. Technol. **19**, 1 (2004).
[16] G. Ali, G. Frosali, and C. Manzini, Ukr. Math. J. **57**, 723 (2005).
[17] L. Barletti, in *Applied and Industrial Mathematics in Italy*, edited by M. Primicerio, R. Spigler, and V. Valente, Series on Advances in Mathematics for Applied Sciences-Vol. 69, Proceedings of the 7th Conference (World Scientific, Singapore, in press).
[18] J. Callaway, *Energy Band Theory* (Academic Press, New York, 1964).
[19] J. M. Luttinger and W. Kohn, Phys. Rev. **97**, 869 (1955).
[20] C. Y. P. Chao and S. L. Chuang, Phys. Rev. B **46**, 4110 (1992).
[21] B. A. Foreman, Phys. Rev. B **54**, 1909 (1996).
[22] E. O. Kane, J. Phys. Chem. Solids **1**, 82 (1956).
[23] N. W. Ashcroft and N. D. Mermin, *Solid State Physics* (Saunders College, Philadelphia, 1976).
[24] W. T. Wenckebach, *Essential of Semiconductor Physics* (J. Wiley & Sons, Chichester, 1999).
[25] E. N. Adams, Phys. Rev. **85**, 41 (1952).
[26] J. H. Davies, *The Physics of Low-Dimensional Semiconductors* (Cambridge University Press, Cambridge, 1998).
[27] P. K. Chakraborty, IEEE Trans. Electron Devices **40**, 214 (1993).
[28] S. L. Chuang, Phys. Rev. B **40**, 10379 (1989).
[29] G. Edwards, E. C. Valadares, and F. W. Sheard, Phys. Rev. B **50**, 8493 (1994).
[30] A detailed discussion of the numerical scheme will be presented in O. Morandi and N. Ben Abdallah (unpublished).
[31] W. R. Frensley, Rev. Mod. Phys. **62**, 745 (1990).
[32] J. Kefi, Ph.D. thesis, Toulouse University, 2003.
[33] R. R. Marquardt, D. A. Collins, Y. X. Liu, D. Z. Y. Ting, and T. C. McGill, Phys. Rev. B **53**, 13624 (1996).
[34] Y. X. Liu, R. R. Marquardt, D. Z. Y. Ting, and T. C. McGill, Phys. Rev. B **55**, 7073 (1997).
[35] A. G. Petukhov, D. O. Demchenko, and A. N. Chantis, Phys. Rev. B **68**, 125332 (2003).
[36] R. Winkler, in *Spin-orbit Coupling Effects in Two-Dimensional Electron and Hole Systems* (Springer-Verlag, New York, 2003).